Regulation of Collective Endothelial Cell Migration by N-cadherin

INTRODUCTION

Collective cell migration involves the coordinated movement of multiple cells that retain cell-cell contacts while coordinating their actin dynamics and intracellular signalling. For this to occur, cells and their neighbours must coordinate with one another by signalling across cell-cell junctions which requires adhesive interactions between cells. In doing so, a leader cell emerges at the front of the cell group and drives migration of follower cells present in the sheet of collectively moving cells and improves the efficiency of their coordinated migratory behaviour (Mayor & Etienne-Manneville, 2016).

There is a wide variety of cell adhesion molecules (Fig. 1). Within these cell adhesion molecules (CAM) an important group are the cadherins. Cadherins depend on calcium ions and are critical for the formation of adherens junctions which allow cell-cell binding. The cadherins can be split into groups (Fig. 2) with our focus being on the Major cadherins and, in particular, on the Type I and Type II classical cadherins. Type I classical cadherins are distinguished by their evolutionarily conserved (Histidine-Alanine-Valine) HAV motif in the first extracellular repeat whereas Type II classical cadherins lack an HAV motif in the first extracellular repeat. Cadherins classified as Type I include CDH -1 (E-cadherin), -2 (N-cadherin), -3 (P-cadherin), -4, -15 and those cadherins classified as Type II include CDH -5 (VE-cadherin), -6, -7, -8, -9, -10, -11, -12, -18, -19, -20, -22, -24. All cadherin isoforms share three main components crucial in their function. On the exterior end, a large extracellular domain composed of a single chain of five tandem glycoprotein repeats serves to mediate cell-cell adhesion contact while a smaller highly conserved C-terminal cytoplasmic domain allows association with actin filaments through catenins such as p120-catenin, beta-catenin, and alpha-catenin (Marie et al., 2014). A small transmembrane component is also present that links the extracellular domain to the intracellular cytoplasmic domain. Along with cadherins, other molecules such as integrins which attach the cell cytoskeleton to the extracellular matrix (ECM) and act as traction sites, and protrusions that extend towards the direction of migration, which include lamellipodia and filopodia, also aid in cell movement. Cadherins are also key modulators in cancer invasion. E-cadherin for example is frequently downregulated in many carcinomas and thus acts as a suppressor. On the other hand, N-cadherin function is more varied. It is known that N-cadherin can act as an invasion promoter in many cancers and can also act as an invasion suppressor such as in osteosarcoma (Derycke & Bracke, 2004). Thus, the upregulation or downregulation of N-cadherin can lead to benign or malignant tumor phenotypes depending on cellular context.

In a previous study, we investigated how expression of E-cadherin (CDH1), normally expressed in epithelial cells, VE-cadherin (CDH5), expressed in endothelial cells, and P-cadherin (CDH3) found in the placenta and expressed in epithelial cells, affect collective migration of Human Umbilical Vein Endothelial Cells (HUVEC). For this study, we continued our previous investigation of collective cell movement with N-cadherin (CDH2) which is expressed in fibroblasts and found in neurons. Neural cell adhesion molecule better known as N-cadherin (CDH2) was first identified

in 1982 (Grunwald, Pratt, & Lilien, 1982) and is now known to be an important player in collective cell migration. The processes of gastrulation and neural crest development during embryogenesis are highly regulated through N-cadherin mediated cell-cell contacts but differ in the type of collective cell movement observed. There is a notion of mass migration in which coordinated movement of a tissue is observed. This is seen in gastrulation where large sheets of cells collectively migrate. In contrast, during neural crest development cells lose contact with each other and may migrate through the ECM as small groups or individually, one after the other, in what is known as chain migration (Derycke & Bracke, 2004). We continued our investigation of collective cell migration in HUVEC expressing N-cadherin and performed experiments with E- and VE-cadherin expressing HUVEC in parallel as controls. We looked at collectively migrating human umbilical vein endothelial cells (HUVEC) to determine how different cadherin isoforms can contribute to cell-cell interactions that affect collective cell behaviour. Our main analysis focused on how cells coordinated their movements with one another in an unperturbed monolayer when plated at varying densities. Ultimately, we were interested in examining the phenotype exhibited by N-cadherin mediated cell-cell contacts in terms of cell coordination between neighbouring cells and understanding the mechanisms behind which cells communicate with each other through extracellular and intracellular signaling interactions and how this leads to their distinct behavior.

Despite functional similarities between different cadherins in how they homotypically bind on the extracellular side and how they connect to the actin cytoskeleton through adaptor proteins intracellularly, different cadherins are expressed in architecturally distinct tissues. Our hypothesis is that specific properties such as strength of homotypic binding between cadherins on the extracellular end and recruitment of adaptor proteins on the intracellular end is paramount for the development of distinct tissue phenotypes. We hope that by understanding the mechanisms behind which cells collectively migrate, we can gain further insight into processes such as morphogenesis, wound healing, embryonic development, and cancer invasion (Friedl & Gilmour, 2009) which all fundamentally rely on coordinated cell movement through cell-cell communication across adherens junctions.

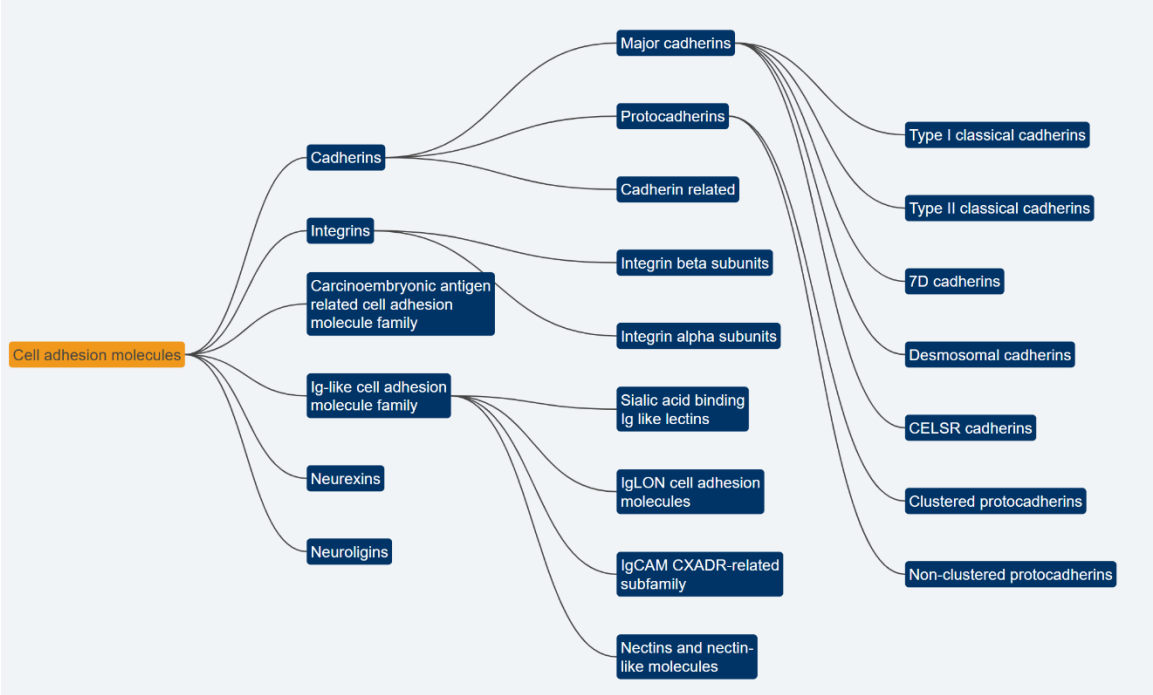

Figure 1. Classification of Cell Adhesion Molecules. Retrieved from https://www.genenames.org/data/genegroup/#!/group/1433

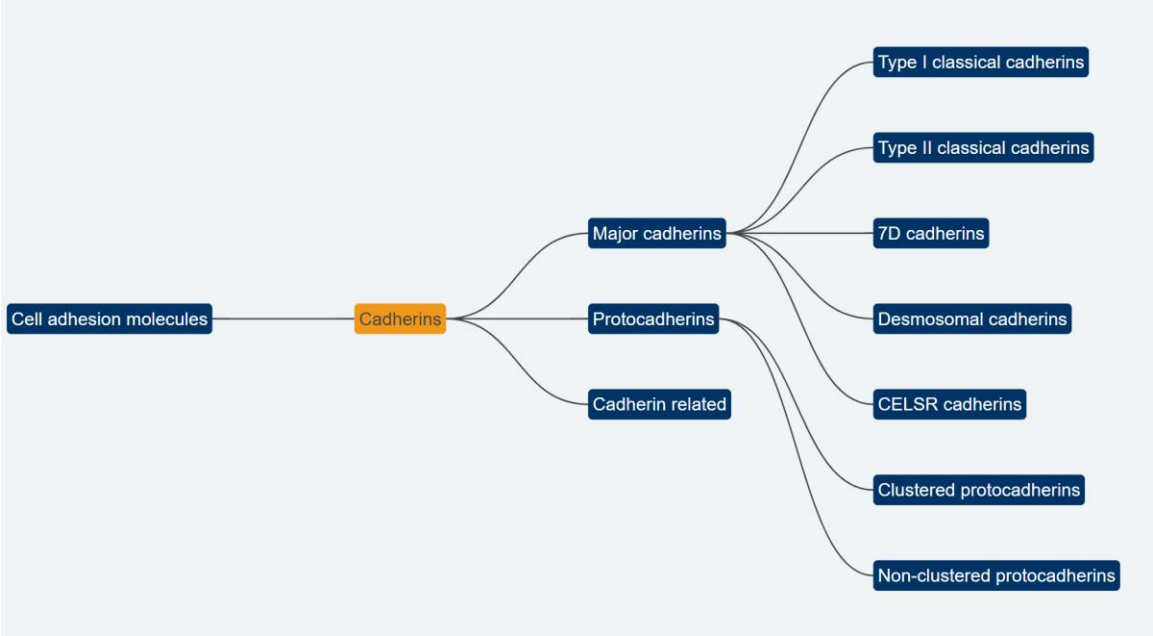

Figure 2. Classification of Cadherins. Retrieved from https://www.genenames.org/data/genegroup/#!/group/16

MATERIALS AND METHODS

Sequence alignment of cadherins. Amino acid sequences of orthologs for VE-, E-, P-, and N-cadherin were downloaded from the Uniprot database. Ortholog sequences used included human, dog, rat, mouse, cow, chicken, and zebrafish. Clustal Omega (https://www.ebi.ac.uk/Tools/msa/clustalo/) was used to perform multiple sequence alignment of all orthologs and results were analyzed in Jalview. For pairwise alignment between VE- and P-cadherin, Benchling's alignment tool was used for analysis.

Cloning of N-cadherin. Forward and reverse primers following standard primer criteria were designed with the Benchling software platform. PCR (31.50 uL ddH2O, 10 uL HF buffer, 1uL dNTPs, 2.5 uL forward-primer, 2.5 uL reverse-primer, 2uL template cDNA, 0.5 uL Phusion DNA Polymerase) and Gel Electrophoresis was performed, and the product was isolated then purified following Gel Extraction. Gibson assembly allowed for the DNA fragments to join and the DNA plasmid was transformed into Mach 1 bacteria grown on LB-Carbenicillin plates. Colonies were selected and incubated in LB and Carbenicillin overnight and the plasmids were extracted following a mini prep protocol. Plasmids were sequenced then produced in large volumes using a Midiprep kit. Endogenously expressed VE-cadherin in HUVEC was replaced by N-cadherin by transducing them with lentivirus encoding N-cadherin.

Cell culture. HUVECs stably expressing VE, E, and N-cadherin isoforms were grown in 6cm plastic dishes and using endothelial growth media ("EndoGRO VEGF" Millipore), endothelial basal media supplemented with fetal bovine serum, growth factors, and L-glutamine. Hygromycin (50 µg/ml) was added to maintain expression of hTERT-IRES-Hygro, and Puromycin (0.5 µg/ml) was added to maintain expression of CDH5-mCitrine-IRES-Puro, E-cadherin-mCitrine-IRES-Puro, and N-cadherin-mCitrine-IRES-Puro.

Cell Fixation and live-cell imaging. Type I Bovine Collagen Solution from Advanced BioMatrix (3mg/ml) was diluted 1:100 with PBS and 100ul of this solution was added to the wells of a glass-bottom 96-well plate. The wells along the perimeter of the plate were unused and coated with 100 ul of diluted collagen solution. The 96-well plate was incubated at 37 ^{o}C overnight or between 16 –24 h after which the collagen solution was aspirated out. Cells were detached from their 6 cm dishes by washing with 5 ml PBS, then 2 ml of trypsin (0.05% Trypsin-EDTA 1X) was added and aspirated out after 30 seconds, and the cells were incubated for 2 min at 37 ^{o}C then resuspended in EndoGRO VEGF. Cells were counted using a hemocytometer and plated at increasing densities of 0.25 x 10^4, 0.5 x 10^4, 1 x 10^4 1.5 x 10^4, and 2 x 10^4 cells per well and incubated at 37 ^{o}C overnight. The wells were then aspirated, and cells were stained with 100 ul Hoechst 33342 nuclear dye diluted 1:50000 (0.2 µg/ml) in growth media and the plate was incubated for 30 min up to 1 h. The staining solution was replaced by 100 ul of LIS (Live-cell imaging solution: 50 ml ECB, 1% FBS, 5 ng/ml bFGF) was added. The plate was sealed with aluminum and incubated for 30 min up to 1 h. Cells were imaged using an automated widefield fluorescence microscope (ImageXpress Micro XLS, Molecular Devices) at 5 min intervals over 25

time points for at total of 2 h using a DAPI-50 filterset and a 4X S Fluor objective. Additional images using a 20X 0.75 NA objective along with a YFP 50 filter set were taken.

Cell density conversion. Microscopy images obtained were analyzed by tracking movement of cell nuclei. The number of cells present in the field of view (FOV) at the start of microscopy was coverted to a cell density in cells per mm^2. Each image was 2160 by 2160 pixels and each pixel had a dimension of 1.62 um by 1.62 um (0.00162 mm). The conversion used was x/(2160*2160*0.00162 x 0.00162) to get cells per mm^2 where x is the number of cells present in the microscopy image FOV.

Cell tracking and motility analysis. Custom written MATLAB functions and scripts were used to automatically track cell nuclei. Movement of nuclei was followed through each time frame by using the nearest neighbour method and cells that left the field of view during microscopy received NaN values from that timepoint onwards. Cells entering the FOV during microscopy would be recorded as a new track with data from that time point onwards and NaN values prior to that time frame. Subsequent time points (5 min intervals) were used to calculate single cell velocity by identifying nuclear displacement from one time point to the next and averaging over 25-time points. Unadjusted single cell velocity was calculated by taking all the data and averaging it while adjusted single cell velocity was calculated only from cells that were present within the FOV during the full 2 h of microscopy and ignoring cells that left or entered the FOV during this time. Coordination of cells was quantitatively analysed using the averaged pairwise velocity correlation between an individual cell and its neighbours within a 100 μm radius (Hayer et al., 2016). The front and rear coordination's of a cell were determined by tracking the nuclei of its neighbouring cells within a 60^o sector in front or behind the cell in question and lateral coordination calculated with cells in the remaining 120^o sectors. Splitting of single cell velocity and coordination was done by segregating data into the first half of and the final half of a time-lapse acquisition.

All code used in this report to analyze data such as coordination and single cell velocity as well as ortholog sequences used in multiple sequence alignment is available upon request.

RESULTS

To investigate how different cadherin isoforms affect collective cell migration, we functionally replaced endogenously expressed VE-cadherin in HUVEC by transducing them with lentivirus encoding E-cadherin and N-cadherin. Localization of classical cadherins at the cell surface is stabilized by association with p120-catenin. In the absence of p120-catenin, cadherins get rapidly internalized (Xiao, Oas, Chiasson, & Kowalczyk, 2007). When exogenous cadherins are (over)expressed in cells, p120-catenin becomes limiting and the exogenously expressed cadherin functionally replaces the endogenous cadherin (Hayer et al., 2016; Xiao et al., 2007).

N-cadherin and E-cadherin expressing cells move faster than VE-cadherin expressing cells

We analyzed the single cell velocity of different cadherin expressing HUVEC as a control for coordination between cells migrating within a monolayer. Our results suggested that VE-cadherin expressing cells generally migrate at a slower rate compared to the N- and E-cadherin expressing cells at all cell densities (Fig 3a). We observed that N-cadherin cells travel at the fastest rate, moving at speeds up to 28 um per hour whereas E-cadherin cells approach 26 um per hour at peak velocity (aside from a possible outlier that reached 28 um per hour), and VE-cadherin cells were the slowest, peaking at 20 um per hour. From Figure 3a, we see that data from both VE-cadherin and E-cadherin expressing cells represent a curved shaped plot where cells move slower at lower densities, reach their highest velocity at densities of ~400 cells mm^{-2}, then begin to slow at higher densities. Furthermore, when splitting the data into two parts with the first part representing data taken from the first hour of microscopy and the second part representing data taken from the second hour of microscopy, we observe an even more pronounced curve for both E-cadherin and VE-cadherin expressing HUVEC (Fig. 3b right). On the other hand, N-cadherin expressing cells appear to migrate at similar rates and even appear to be increasing in speed as cell densities increase with single cell velocity ranging between 24 and 28 um per hour.

a

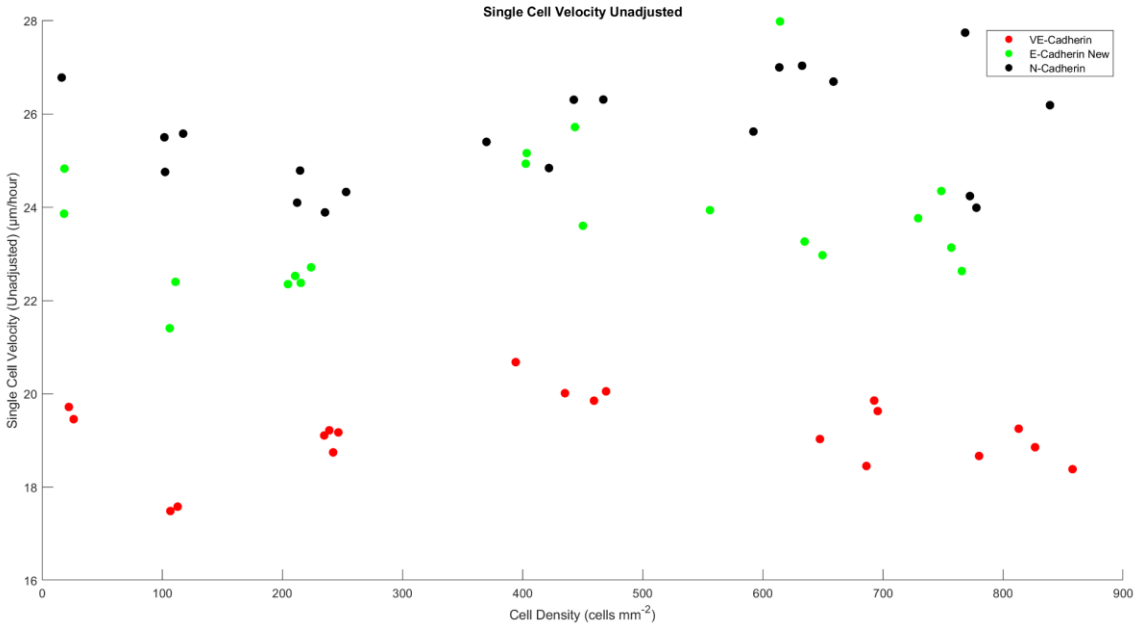

b

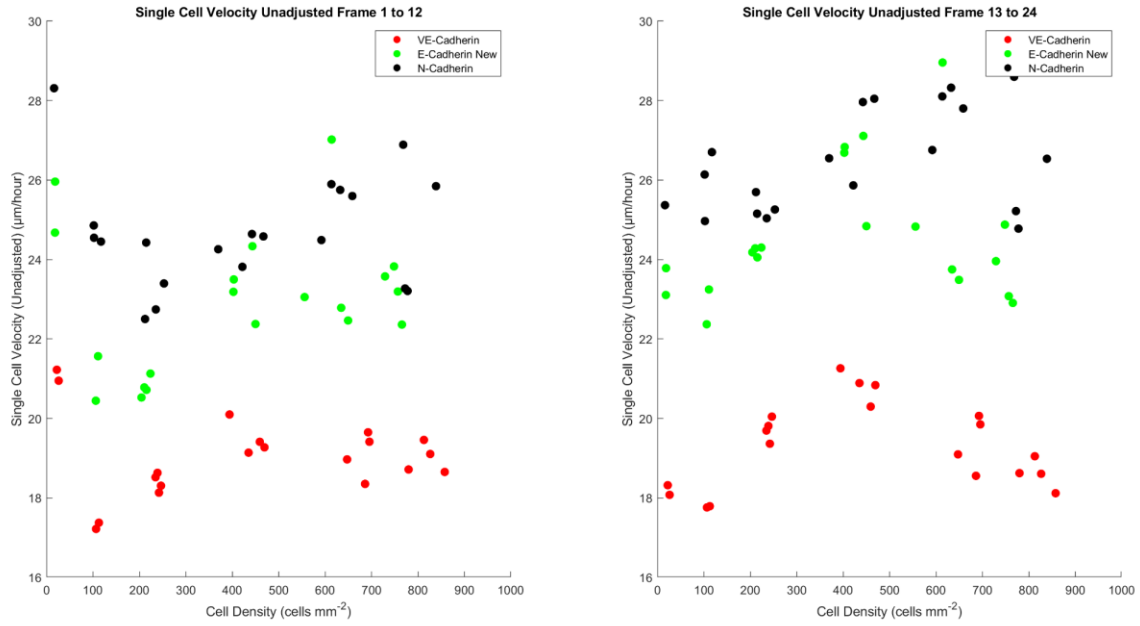

Figure 3. Single cell velocity analysis of VE-cadherin, E-cadherin and N-cadherin-expressing HUVEC in an unperturbed monolayer. Each data point corresponds to the averaged velocity of cells in an entire well of a 96-well plate and corresponds to one experiment. **(a)** The single cell velocity of cells over 2 hours of imaging and **(b)** The single cell velocity of cells split between the first hour of microscopy imaging (left) and the second hour of imaging (right) as a function of cell density.

E-cadherin and N-cadherin have similar average coordination across all cell densities.

In terms of coordination between cells, our data demonstrates that there is no clear difference between E-cadherin and N-cadherin expressing cells in how coordinated they are across different cell densities (Fig. 4a). Aside from E-cadherin cells having slightly higher coordination at cell densities below 200 cells per mm^{-2}, they are generally indistinguishable from one another. VE-cadherin expressing cells are the most coordinated and interestingly, their coordination across different densities is almost identical to the curve seen for their single cell velocity. For all three cadherin types, cells plated at ~400 cells per mm^{-2} showed highest coordination. We then split the data into the coordination results from the first hour of microscopy (Fig. 4b left) and the results from the second hour of microscopy (Fig. 4b right) to gain a better representation of cell behavior. The basis being that cells may have still been adjusting to new conditions and not had time to settle when imaged under the miscroscope. We see that in the first hour of microscopy, N-cadherin and E-cadherin expressing cells seem to be less similarly coordinated, but data from the second hour of miscroscopy suggests that their coordination across different cell densities is in fact almost identical. Furthermore, whereas data from the full 2 hour microscopy (Fig. 4a) showed that E-cadherin cells were slightly more coordinated at lower densities, data from the second hour of microscopy (Fig 4b right) argues instead that they are similarly coordinated. Alongside this we also see VE-cadherin expressing HUVEC being more coordinated at their optimal cell density of 400 – 500 cells per mm^{-2} during the second hour of microscopy supporting our reasons for splitting the data for analysis.

At densities above 400 cells per mm^{-2}, front coordination between all three cadherin (VE-, E-, N-) expressing HUVEC show similar trends.

The front coordination was calculated by taking neighbours located within a 60^{o} sector in front of the cell of interest and results were quite different from the overall coordination values. In the front coordination (Fig. 4c), we observe that when cells are plated at densities greater than 400 cells per mm^{-2}, front coordination for all cadherin expressing HUVEC begins to decrease and front coordination between the different cadherins becomes hard to distnguish between. At the cell density region (densities of 100 cells per mm^{-2} and lower), N-cadherin expressing cells are generally better coordinated at the front with VE-cadherin expressing cells being the least coordinated. However, at 200 cells per mm^{-2}, all different cadherin expressing HUVECs become similarly coordinated at their front. The rear coordination was calculated by taking neighbours within a 60^{o} sector behind the cell of interest and for cells plated at densities above 400 cells per mm^{-2}, our results show that all three different cadherin expressing cells are almost identically coordinated (Fig. 4e). However, peculiarly, at densities below 400 cells per mm^{-2}, N-cadherin expressing cells are less coordinated at the rearin comparison to VE- and E-cadherin expressing HUVEC. The front, lateral and rear coordinations were split into the first hour of microscopy (Fig. 4f top) and second hour of microscopy (Fig. 4f bottom) to get a clearer representation of coordinated movements between cells. From the second hour of microscopy (Fig. 4f bottom),

we observe that N-cadherin and E-cadherin expressing cells are more alike and show similar trends in front and rear coordination in comparison to VE-cadherin expressing cells. The axes were adjusted so that the limits were along the same range (Fig. 4g) to show the difference between coordinated movements in the front, lateral, and rear of cells with respect to one another.

N-cadherin expressing cells are less laterally coordinated than VE-cadherin and E-cadherin HUVECs

The lateral coordination was calculated from neighbours within the regions between the front and rear (Fig. 4d). At densities above 400 cells per mm^{-2}, cells expressing N-cadherin were less laterally coordinated than both VE- and E-cadherin and had lateral coordination scores between 0.025 and 0.05. As with front and rear coordination, cells expressing VE-cadherin had the highest lateral coordination at this density region, reaching 0.07, while E-cadherin expressing cells were in between N- and VE-cadherin expressing cells in terms of coordination scores. At densities below 400 cells per mm^{-2}, lateral coordination values were almost identical between the different cell types and indiscernible.

a

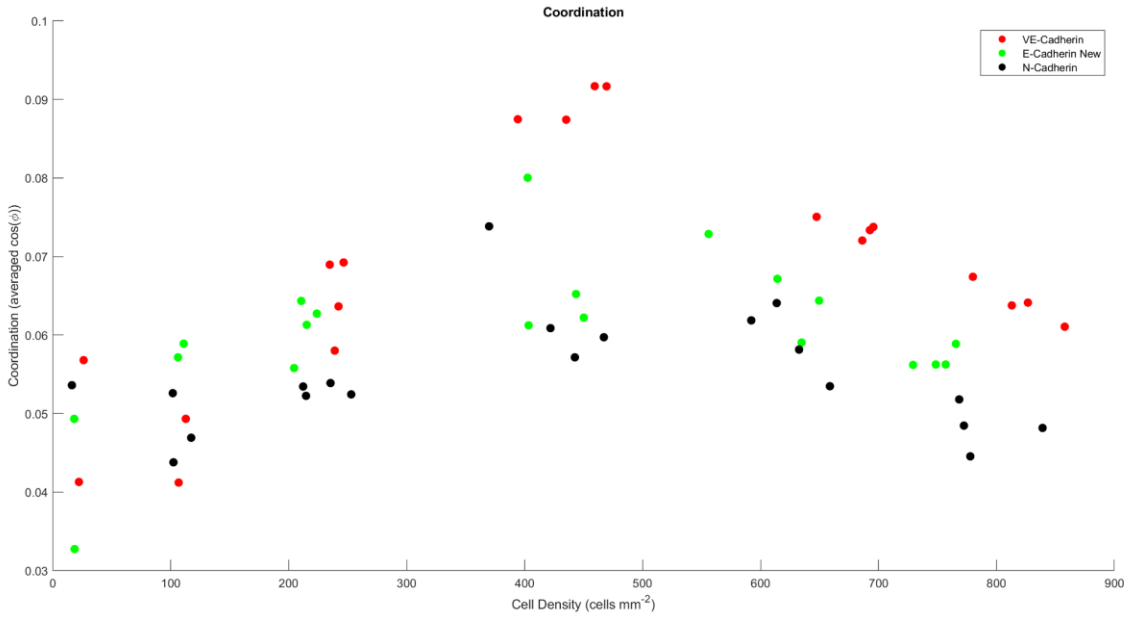

b

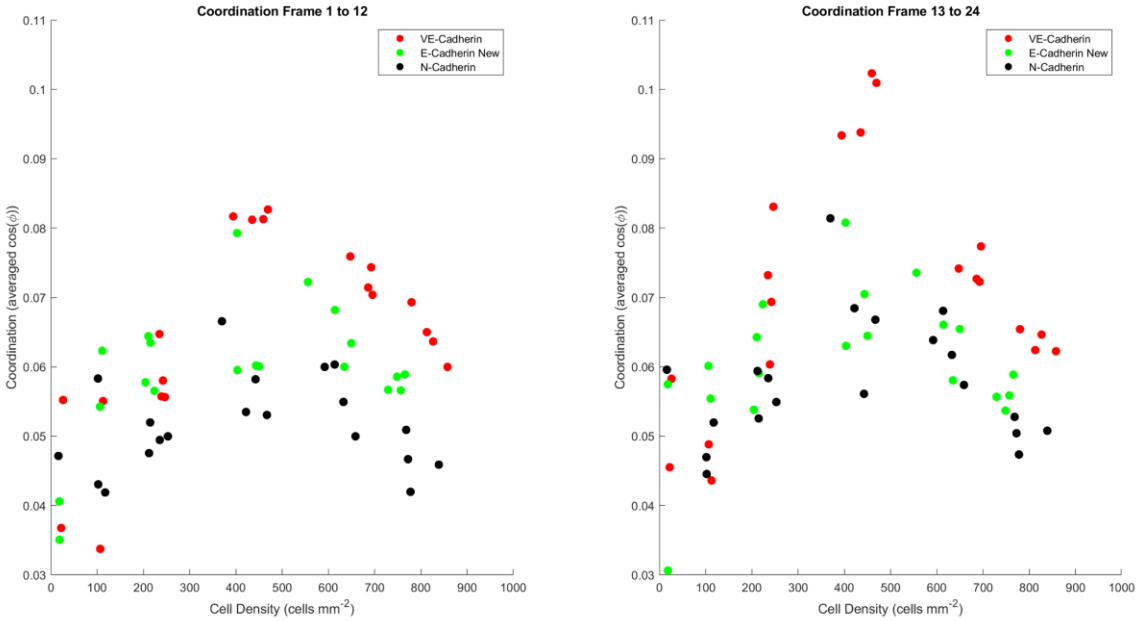
Coordination Frame 1 to 12
VE-Cadherin
E-Cadherin New
N-Cadherin
Coordination (averaged cos(φ))
Cell Density (cells mm-2)
Coordination Frame 13 to 24
VE-Cadherin
E-Cadherin New
N-Cadherin
Coordination (averaged cos(φ))
Cell Density (cells mm-2)

c

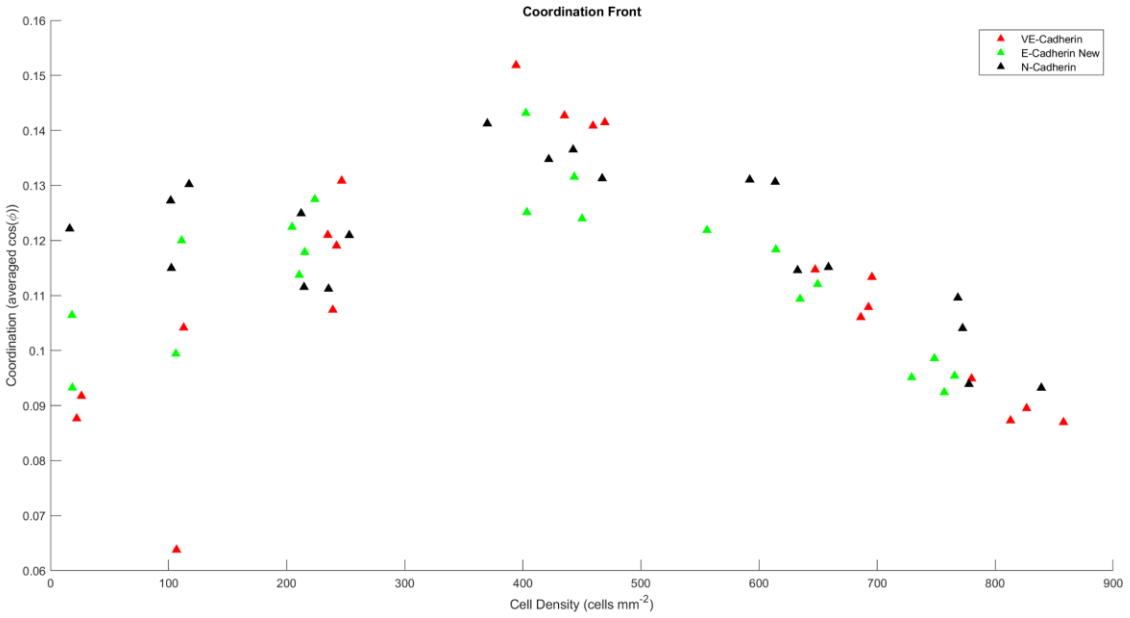
Coordination Front
VE-Cadherin
E-Cadherin New
N-Cadherin
Coordination (averaged cos(φ))
Cell Density (cells mm-2)

d

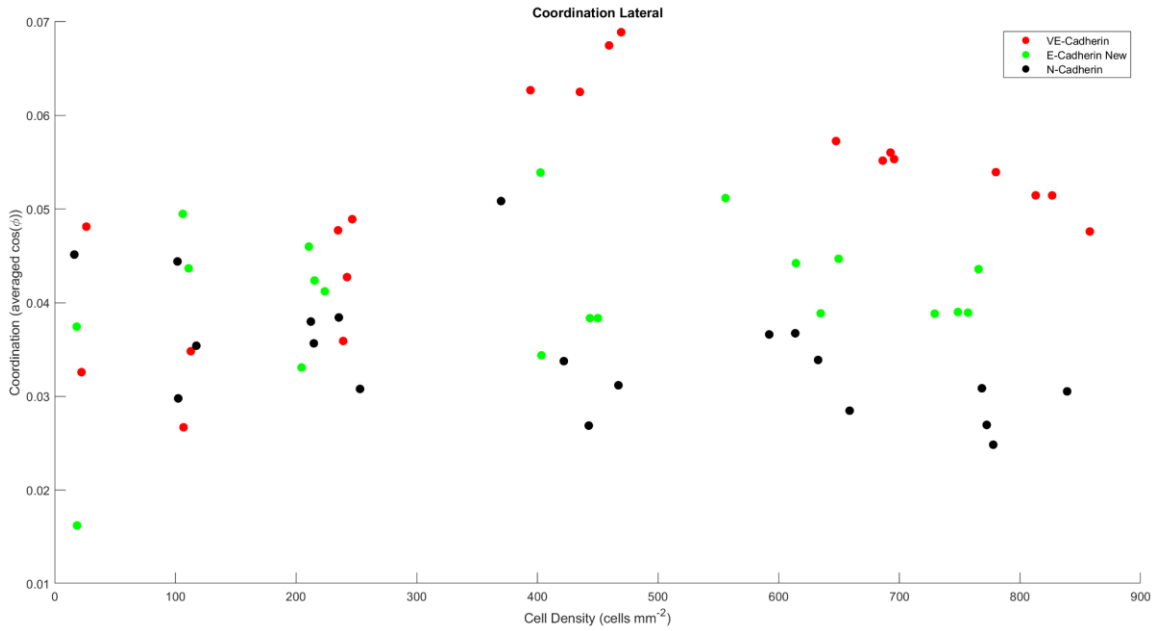
Coordination Lateral
VE-Cadherin
E-Cadherin New
N-Cadherin
Coordination (averaged cos(φ))
Cell Density (cells mm^{-2})
0.07
0.06
0.05
0.04
0.03
0.02
0.01
0
100
200
300
400
500
600
700
800
900

e

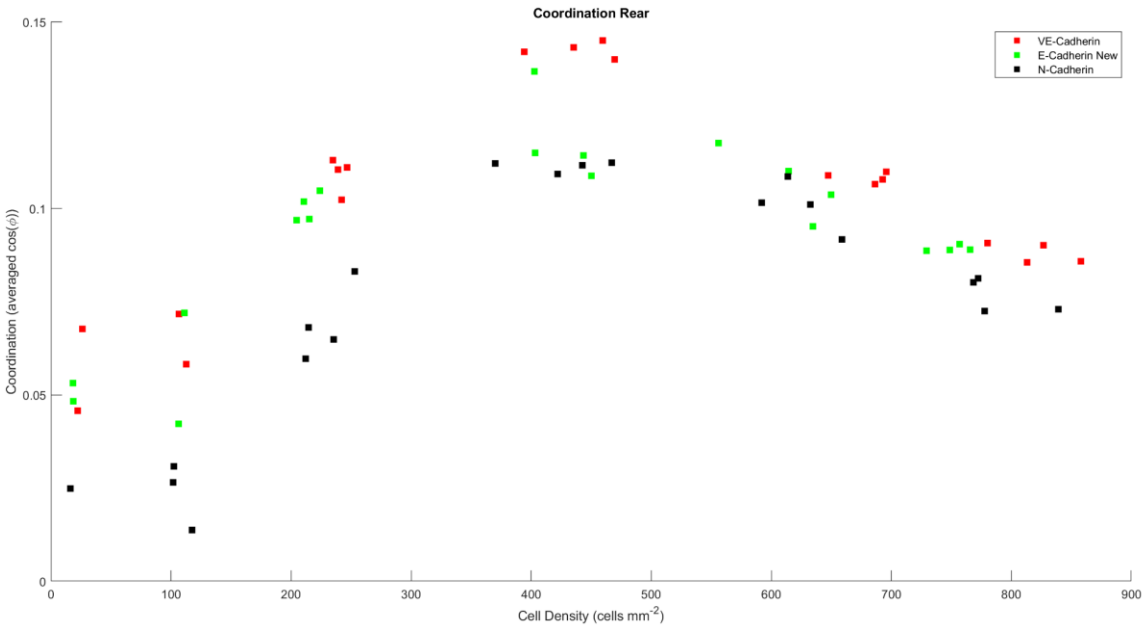
Coordination Rear
VE-Cadherin
E-Cadherin New
N-Cadherin
Coordination (averaged cos(φ))
Cell Density (cells mm^{-2})
0.15
0.1
0.05
0
100
200
300
400
500
600
700
800
900

f

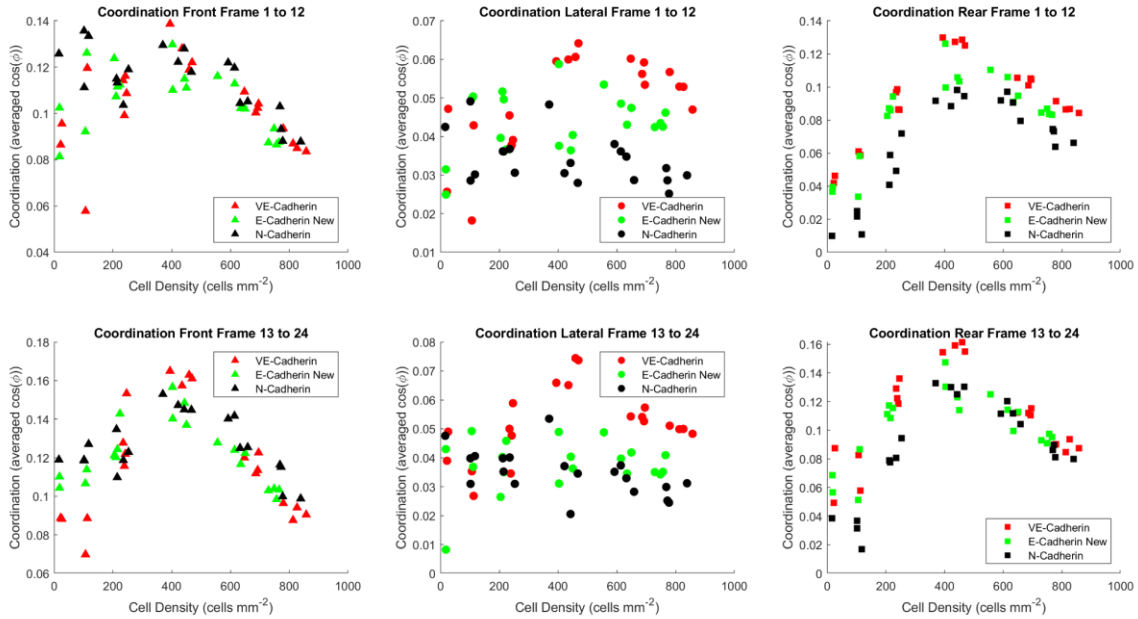

g

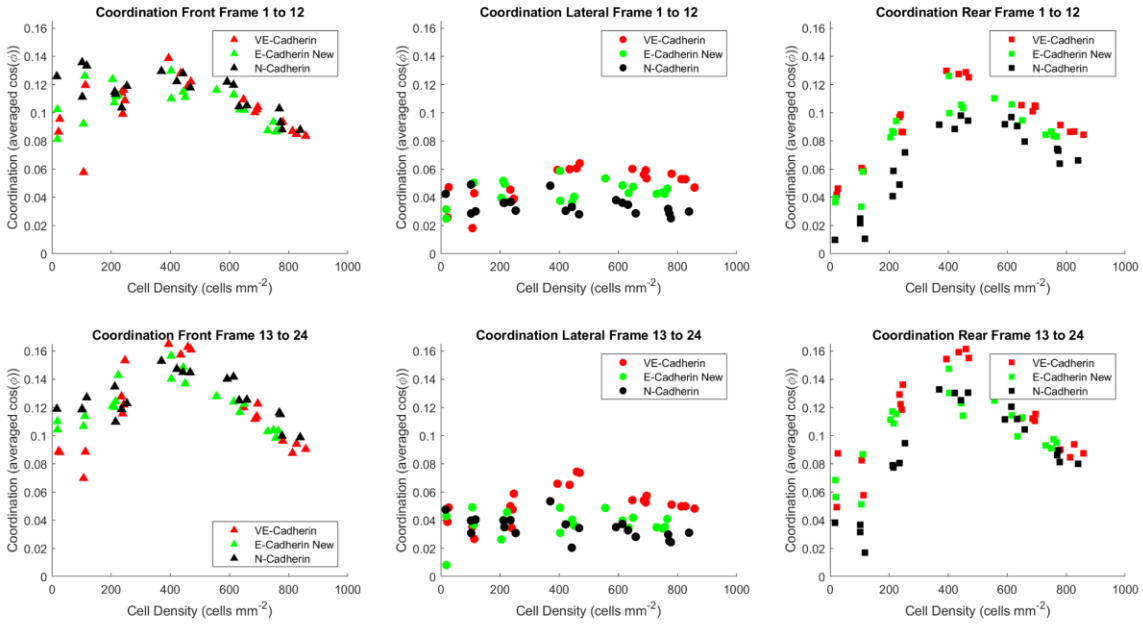

Figure 4 Coordination scores as a function of cell density in unperturbed monolayers. Each data point represents the averaged coordination values of all cells within an entire well and correspond to a single experiment. **(a)** The coordination values of each VE-, E-, and N-cadherin plated at different densities. **(b)** The coordination values of cells split between the first hour of microscopy imaging (left) and the second

hour of imaging (right) as a function of cell density. Front **(c)**, lateral **(d)**, and rear **(e)** coordination values were calculated by taking neighbours present in a 60^o sector in the front, 120^o sector on the sides, and 60^o sector in the back of a cell, respectively. **(f)** The front (left), lateral (middle) and rear (right) coordinations split into the first half of microscopy (top) and second half of microscopy (bottom) and **(g)** controlling for the axis limits.

DISCUSSION & LIMITATIONS

At low cell densities, migration behavior appears to be stochastic, but at higher cell densities cells begin to influence the behavior of one another. Our data argue that at lower cell densities (below 300 cells per mm^2), cells are less confluent within the monolayer and this results in less cell-cell contact between neighbouring cells. A consequence is less cell-cell adhesion between cells and therefore less collective migratory behavior which results in more uncoordinated cell behavior. An interesting phenomenon is that, for all three cadherin expressing cell types, peak average coordination is observed at ~400 cells per mm^2 which may suggest that at higher densities, physical interactions may come into play. For example, at higher cell densities (above 600 cells per mm^2), cells may be too confluent and when collectively migrating, may end up interfering with one another resulting in slower speeds and less coordinated behaviour. Our results demonstrate that for VE- and E-cadherin expressing HUVEC, coordination seems to be positively correlated with single cell velocity such that at lower speeds, coordination between cells is lower and at higher speeds, cells are better coordinated with their neighbours. In contrast, N-cadherin expressing cells do not show similar correlation between their single cell velocity and coordination, as they are most coordinated at 400 cells per mm^2 while peak single cell velocity is reached at ~600 cells per mm^2. For all cell types, in terms of the front and rear coordination in comparison to lateral coordination, we observed that cells were more coordinated at their front and rear as opposed to with cells at their sides as observed previously (Hayer et al., 2016). Additionally, our data argues that E-cadherin and N-cadherin expressing HUVEC show more similarity with one another in terms of front and rear coordination than VE-cadherin expressing cells and often are almost indistinguishable (Fig. 4f bottom).

A possible explanation for this difference may be the presence or absence of HAV repeats. It is known that in vertebrates, Type I classical cadherins such as E- and N-cadherin contain a Histidine79—Alanine80—Valine81 (HAV) sequence in the first cadherin EC1 domain that is evolutionarily conserved whereas the Type II classical cadherins in vertebrates do not contain the HAV sequence in the first repeat. Studies have shown that cis interactions are promoted by the His79 and Ala80 residues while the Val81 part of the sequence is responsible for trans interactions (Bunse et al., 2013; Harrison et al., 2011). The tryptophan binding pocket contains the Ala80 residue which is able to dock a tryptophan (Tryp2) residue on the N-terminus EC1 domain of another N-cadherin which facilitates intercellular adhesion (Fig. 5) (Blaschuk, 2015). It has also been shown that N-cadherin (CDH2 Type I cadherin) function can be inhibited by these short HAV peptides. Furthermore, the activity and specificity of the HAV peptides is affected by the amino acids flanking the HAV sequence. For instance, when the HAV motif has a single aspartic acid flanking it, the peptide becomes more effective at inhibiting N-cadherin function. This is a result of the single aspartic acid mimicking the natural N-cadherin HAVD sequence. On the other hand, when a single serine flanks the HAV motif, the peptide is unable to inhibit N-cadherin function since the serine mimics the natural E-cadherin HAVS sequence (Williams, Williams, Gour, Blaschuk, & Doherty, 2000).

As mentioned prior, it is known that extracellular interactions between classical cadherins occurs through engagement of their individual EC1 ectodomains. The EC1 domains are able to swap or exchange their N-terminal beta-strands through homophilic-trans interactions (Harrison et al., 2010). Through this exchange, a dimer can be formed and is stabilized by the Trp2 residue on the EC1 domain of one cadherin being positioned in the hydrophobic pocket of the EC1 domain of the partner cadherin. Additional stability is conferred by interactions between residues flanking Trp2 as well as interactions between regions within the EC1 domain of one cadherin with the EC2 domain of another cadherin through lateral cis interactions (Saito & Dana, 2012). The overall stability of these junctional interactions is maintained by cooperativity between the strong trans-dimers and weak cis-interactions (Harrison et al., 2011; Saito & Dana, 2012). Within the EC1 domains of cadherins, the interface between the interaction of Type II cadherin N-terminal beta strands consists of two conserved tryptophan side chains that anchor each swapped strand whereas Type I cadherins (N-, E-cadherin) only have one which may play a role in explaining why at higher densities VE-cadherin expressing cells show higher coordination than E- and N-cadherin expressing cells. Furthermore, the interface in Type II cadherins are unique in the presence of their large hydrophobic regions (Patel et al., 2006). Furthermore, it has been shown that most cadherins, other than classical Type I, II and desmosomal cadherin EC1 domains, have domains that do not bind through a strand-swapping mechanism and most likely utilize separate protein-protein interaction interfaces (Posy, Shapiro, Honig, & Eye, 2008).

In terms of single cell velocity, the increased speed of N-cadherin expressing HUVEC may be explained by a domain present within the EC4 extracellular part of the cadherin. Prior studies have identified a 69 amino acid part of the EC4 domain of N-cadherin that results in increased motility that is unassociated with cell-cell adhesion which supports and provides evidence for the independence of cell adhesion from cell motility (Kim et al., 2000). This is consistent with our data as we see that N-cadherin expressing HUVEC appear to maintain their single cell velocity at high densities (above 400 cells per mm^{-2}) and even appear to be increasing in speed while coordination begins to level off and decline.

A limitation for this study includes the undetermined expression levels of the N-cadherin that is being aberrantly expressed within HUVEC. Earlier studies showed that when Type I and Type II cadherins were being expressed at similar expression levels, Type I cadherin-expressing cells adhered not only more quickly but also more strongly than Type II cadherin expressing cells. Moreover, it was found that the complexes formed between Type II cadherins and Beta-catenin are less stable. With the help of chimeric cadherins, it was also discovered that cell adhesivity was predominantly affected by the extracellular domain (Chu et al., 2006). Since from our results, we observed that VE-cadherin (a Type II cadherin) is actually (slightly) more coordinated than the Type I cadherins tested (E- and N-cadherin), other intracellular adaptors (for example Fer, which interacts with p120-catenin) and upstream and downstream regulators must be involved and the stronger and faster cell adhesive properties of Type I cadherins may play a role but may not be the main determining factor in whether cells are more coordinated with one another.

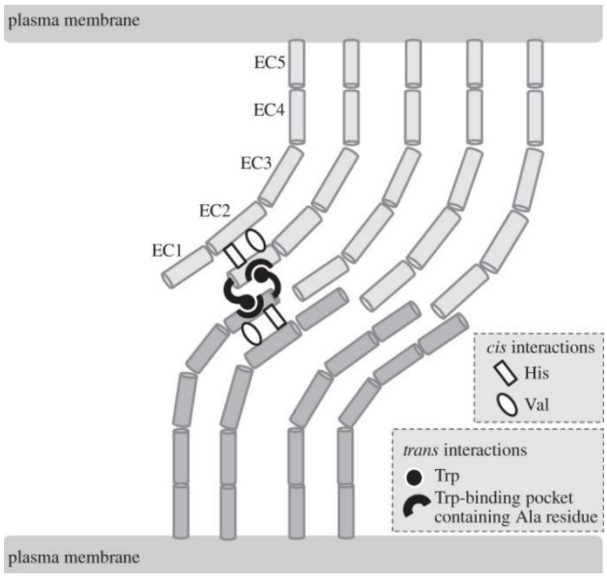

Figure 5 Interaction between extracellular domains of N-cadherin EC1 extracellular domains showing the HAV sequences and their interaction with tryptophan. Retrieved from (Blaschuk, 2015). https://www.ncbi.nlm.nih.gov/pmc/articles/PMC4275908/figure/RSTB20140039F1/

FUTURE DIRECTIONS

We have begun domain swapping of extracellular and intracellular domains of different cadherins to create chimeras to test the effect on coordination. Currently we are working on cloning a chimera composed of a CDH3 (P-cadherin) extracellular domain connected to a CDH5 (VE-cadherin) intracellular domain and in the near future we plan to create another chimera composed of a CDH5 extracellular domain joined to a CDH3 intracellular domain.

Prior to deciding on the chimeras to create, we performed sequence alignment analyses to determine which cadherins to create chimeras from. We looked at Multiple sequence alignment results in Jalview for orthologs of E-cadherin, VE-cadherin, N-cadherin, and P-cadherin. Our results (from the previous report) showed that P-cadherin expressing cells had front coordination values that diverged from the VE- and E-cadherin expressing HUVEC. However, when looking at results from our Multiple sequence alignment (not shown), we observed that E-cadherin and P-cadherin seemed very similar in their protein sequences while the VE-cadherin sequence diverged from the rest.

We determined that creating chimeras of E- and P-cadherin would be a better choice since their sequences were similar, and they showed distinct phenotypes in terms of their coordination. On the other hand, the VE-cadherin sequence was distinct from the P-cadherin sequence and both also displayed distinct phenotypes, but the difficulty would lie in narrowing down the region that was causing the phenotype difference as there were too many distinct regions in the sequence. We performed further analysis (pairwise comparison) of the intracellular domain sequence region of P-cadherin and E-cadherin. We focused on the intracellular region rather than the extracellular domain since most of the signalling as well as adaptor and effector binding occur in this region. Also, we would have less capability of investigating the extracellular domain since we would be looking at mechanical binding. From our analysis, we concluded that there would not be any difference in phenotype if we performed a domain swap (created chimeras with E-cadherin intracellular domain and P-cadherin extracellular domain and vice versa) since the intracellular domains looked almost identical in both the P-cadherin and E-cadherin. Thus, we decided to proceed with chimeras composed of VE-cadherin and P-cadherin.

Another future investigation would be to determine whether other cadherins other than VE-cadherin contained cadherin fingers. From 20X microscopy images of VE-, N-, and E-cadherin (Fig. 6 a, b, c respectively), we observed that VE-cadherin cells showed highest expression levels within junctional regions and E-cadherin expressing cells displayed the lowest expression levels while N-cadherin expressing cells were in between the two.

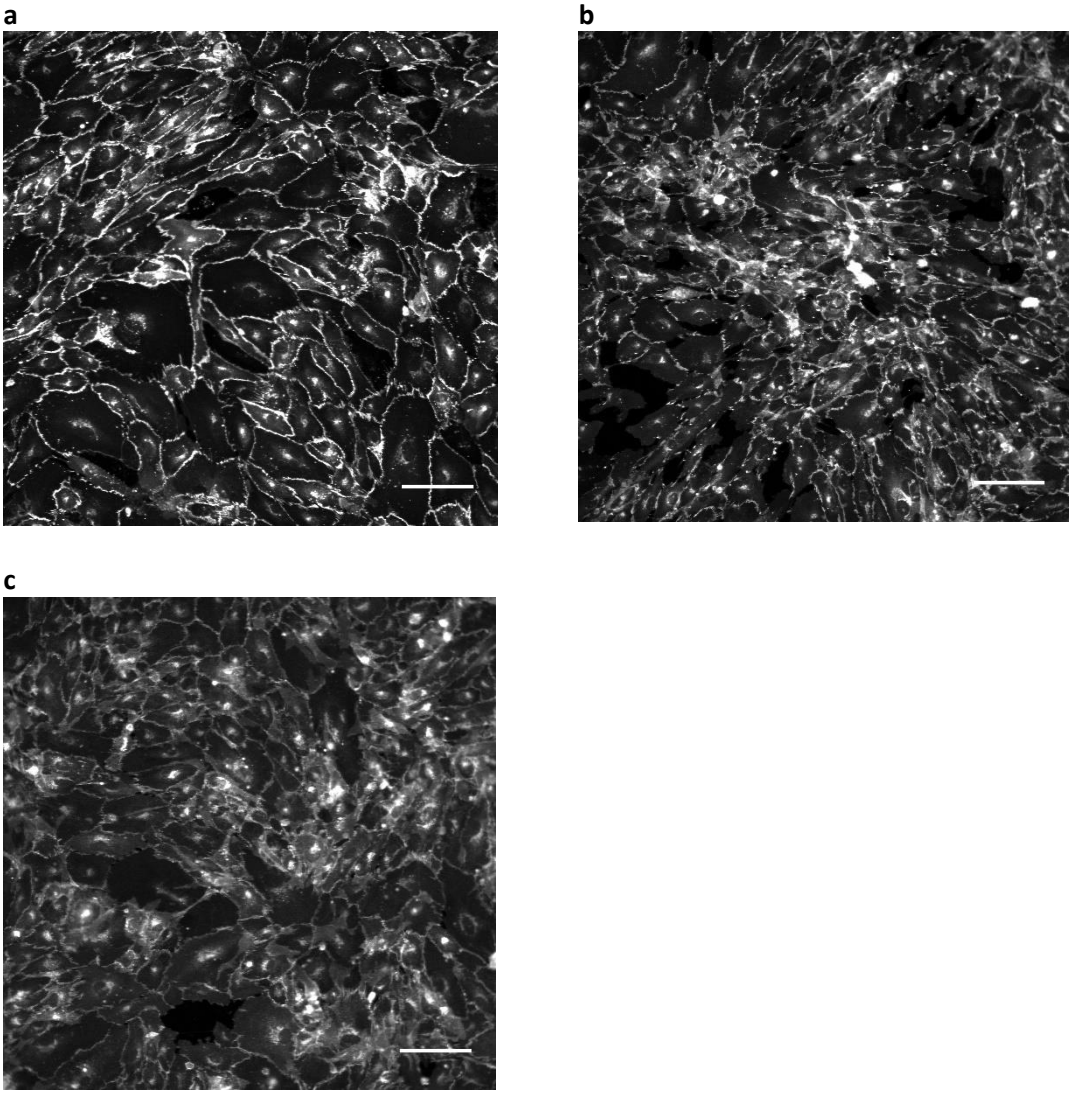

Figure 6 20X images of cadherin expressing HUVEC imaged with a 0.75 NA objective along with a YFP50 filter set. All images are from cells plated at 10k cells per ml. **(a)** VE-cadherin cells **(b)** N-cadherin cells and **(c)** E-cadherin cells. Scale Bar, 100 um.

ACKNOWLEDGEMENTS

I am grateful for all members of the Hayer lab for providing an interactive and supportive environment in which knowledge and ideas can flow and I am extremely thankful for Arnold Hayer for his time, commitment, and patience and for allowing me to continue my investigation into cadherins and their role in collectively migrating cells within his lab. I also thank the Biology Department at McGill for giving me this wonderful opportunity to conduct research under the guidance of a fantastic and brilliant researcher.

REFERENCES

Blaschuk, O. W. (2015). N-cadherin antagonists as oncology therapeutics. *Philosophical Transactions of the Royal Society B: Biological Sciences*, *370*(1661), 8–11. https://doi.org/10.1098/rstb.2014.0039

Bunse, S., Garg, S., Junek, S., Vogel, D., Ansari, N., Stelzer, E. H. K., & Schuman, E. (2013). Role of N-cadherin cis and trans interfaces in the dynamics of adherens junctions in living cells. *PLoS ONE*, *8*(12), 1–16. https://doi.org/10.1371/journal.pone.0081517

Chu, Y., Eder, O., Thomas, W. A., Simcha, I., Pincet, F., Ben-ze, A., … Dufour, S. (2006). Prototypical Type I E-cadherin and Type II Cadherin-7 Mediate Very Distinct Adhesiveness through Their Extracellular Domains * □, *281*(5), 2901–2910. https://doi.org/10.1074/jbc.M506185200

Derycke, L. D. M., & Bracke, M. E. (2004). <Ncad adhesion review.pdf>, *476*, 463–476.

Friedl, P., & Gilmour, D. (2009). Collective cell migration in morphogenesis, regeneration and cancer. *Nature Reviews Molecular Cell Biology*, *10*(7), 445–457. https://doi.org/10.1038/nrm2720

Grunwald, G., Pratt, R., & Lilien, J. (1982). Enzymic Dissection of Embryonic Cell Calcium-Dependent Adhesive System of Embryonic Chick Neural Retina. *Journal of Cell Science*, *83*(1981), 69–83.

Harrison, O. J., Bahna, F., Katsamba, P. S., Jin, X., Brasch, J., Vendome, J., … Shapiro, L. (2010). Two-step adhesive binding by classical cadherins, *17*(3). https://doi.org/10.1038/nsmb.1784

Harrison, O. J., Jin, X., Hong, S., Bahna, F., Brasch, J., Wu, Y., … Honig, B. (2011). NIH Public Access, *19*(2), 244–256. https://doi.org/10.1016/j.str.2010.11.016.The

Hayer, A., Shao, L., Chung, M., Joubert, L. M., Yang, H. W., Tsai, F. C., … Meyer, T. (2016). Engulfed cadherin fingers are polarized junctional structures between collectively migrating endothelial cells. *Nature Cell Biology*, *18*(12), 1311–1323. https://doi.org/10.1038/ncb3438

Kim, J. B., Islam, S., Kim, Y. J., Prudoff, R. S., Sass, K. M., Wheelock, M. J., & Johnson, K. R. (2000). N-cadherin extracellular repeat 4 mediates epithelial to mesenchymal transition and increased motility. *Journal of Cell Biology*, *151*(6), 1193–1205. https://doi.org/10.1083/jcb.151.6.1193

Marie, P. J., Haÿ, E., Modrowski, D., Revollo, L., Mbalaviele, G., & Civitelli, R. (2014). Cadherin-mediated cell-cell adhesion and signaling in the skeleton. *Calcified Tissue International*, *94*(1), 46–54. https://doi.org/10.1007/s00223-013-9733-7

Mayor, R., & Etienne-Manneville, S. (2016). The front and rear of collective cell migration. *Nature Reviews Molecular Cell Biology*, *17*(2), 97–109. https://doi.org/10.1038/nrm.2015.14

Patel, S. D., Ciatto, C., Chen, C. P., Bahna, F., Rajebhosale, M., Arkus, N., … Price, S. R. (2006).

Type II Cadherin Ectodomain Structures : Implications for Classical Cadherin Specificity, 1255–1268. https://doi.org/10.1016/j.cell.2005.12.046

Posy, S., Shapiro, L., Honig, B., & Eye, E. S. H. (2008). Sequence and Structural Determinants of Strand Swapping in Cadherin Domains : Do All Cadherins Bind Through the Same Adhesive Interface ?, 954–968. https://doi.org/10.1016/j.jmb.2008.02.063

Saito, M., & Dana, K. (2012). Classical and desmosomal cadherins at a glance, *066654*, 2547–2552. https://doi.org/10.1242/jcs.066654

Williams, E., Williams, G., Gour, B. J., Blaschuk, O. W., & Doherty, P. (2000). A Novel Family of Cyclic Peptide Antagonists Suggests That N-cadherin Specificity Is Determined by Amino Acids That Flank the HAV Motif *, *275*(6), 4007–4012.

Xiao, K., Oas, R. G., Chiasson, C. M., & Kowalczyk, A. P. (2007). Role of p120-catenin in cadherin trafficking. *Biochimica et Biophysica Acta - Molecular Cell Research*, *1773*(1), 8–16. https://doi.org/10.1016/j.bbamcr.2006.07.005

Figures

Figure 2. Classification of Cadherins. Retrieved from https://www.genenames.org/data/genegroup/#!/group/16

Figure 2. Classification of Cadherins. Retrieved from https://www.genenames.org/data/genegroup/#!/group/16

SUPPLEMENTARY FIGURES

Figure S1 Single cell velocity analysis of VE-cadherin (red), E-cadherin (green) and N-cadherin (black) expressing cells in an unperturbed monolayer with data calculated only from cells present in the FOV during the entire microscopy period. Cells leaving or entering the FOV at different time points during microscopy were exluded from the calculation. **(a)** The overal single cell velocity averaged over 2 hours and **(b)** single cell velocity split between the first hour of microscopy (left) and the second hour of microscopy (right) as a function of cell density.

a

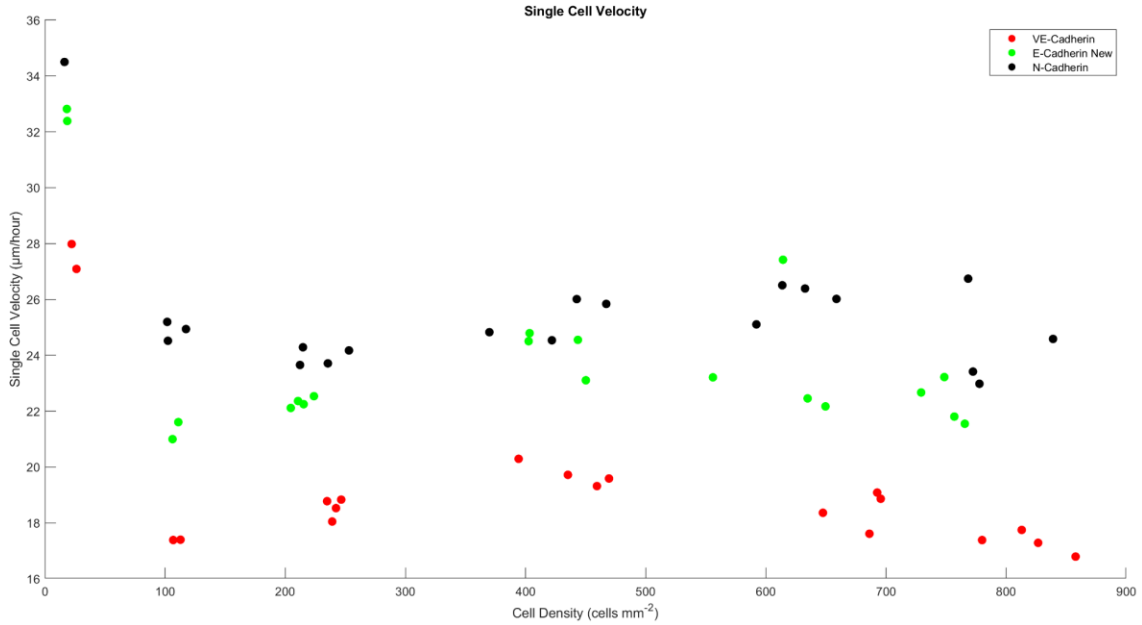

b